TEPORINGOS

TrEatment of PhOtoionized Regions IN Glamorous ObjectS

V. Gómez-Llanos[1], V. Fernández[2], Z. Zhang[3], K. Z. Arellano-Códova[2], L. Juan de Dios[2] and G. Domínguez-Guzmán[2]

[1]Instituto de Astronomía, Universidad Nacional Autónoma de México, Mexico; [2]Instituto Nacional de Astrofísica, Óptica y Electrónica, Puebla, Mexico; [3]Institute University of Georgia, USA.

Abstract

We explore the cause of the very high He II $\lambda4686$ /Hβ = 15.23 (Hβ = 100) observed in the H II region N44C using grids of photoionization models with CLOUDY (Ferland et al. 2017). We constrain the possible ionization source and the physical parameters for N44C. Furthermore, we extend our model to the PDR and the molecular phase, to analyze the molecular abundances rovibrationaly. The results show that a high energy source is necessary to reproduce the observed lines.

Introduction

N44C is a H II region at 50 kpc in the Large Magellanic Cloud (LMC). The physical properties of this object are: average n_e of 140 cm^{-3}, T_e([O III]) and T_e([N II]) are 11300 K and 10400 K, respectively. This H II region is peculiar because its spectrum has He II lines unexpected for this kind of objects, specially since the ionizing source is an O7 (Garnett et al. 2000).

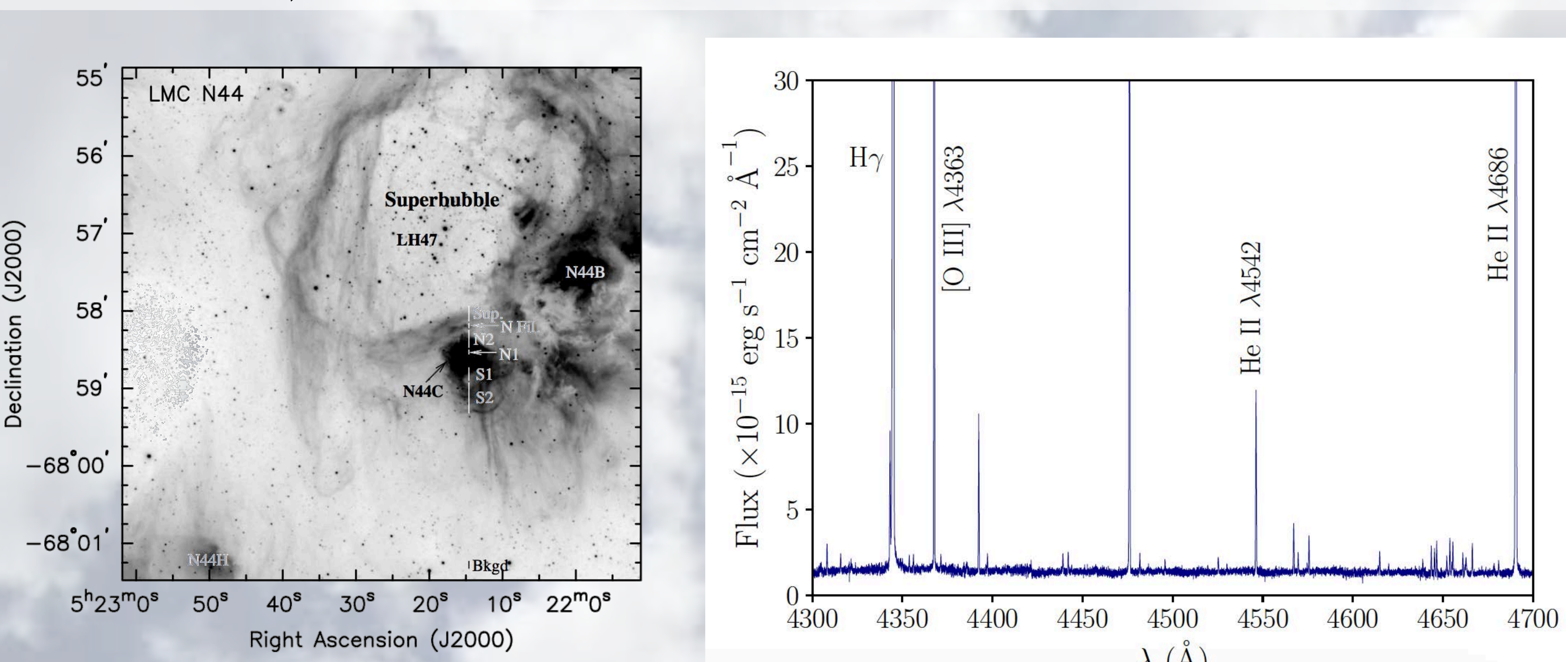

Figure 1. Left: image of N44C, figure taken from Nazé et al. (2003). Right: part of the spectrum of N44C where He II emission lines are detected.

Models

We construct two grids of photoionization models with CLOUDY using two different stellar atmosphere models, Krupa (Martín-Majón et al. 2010) and Tlusty (Lanz & Hubeny 2007). Table 1 shows the parameters used to construct each grid of models. We select the stellar atmosphere models of Tlusly according to Figure 1.

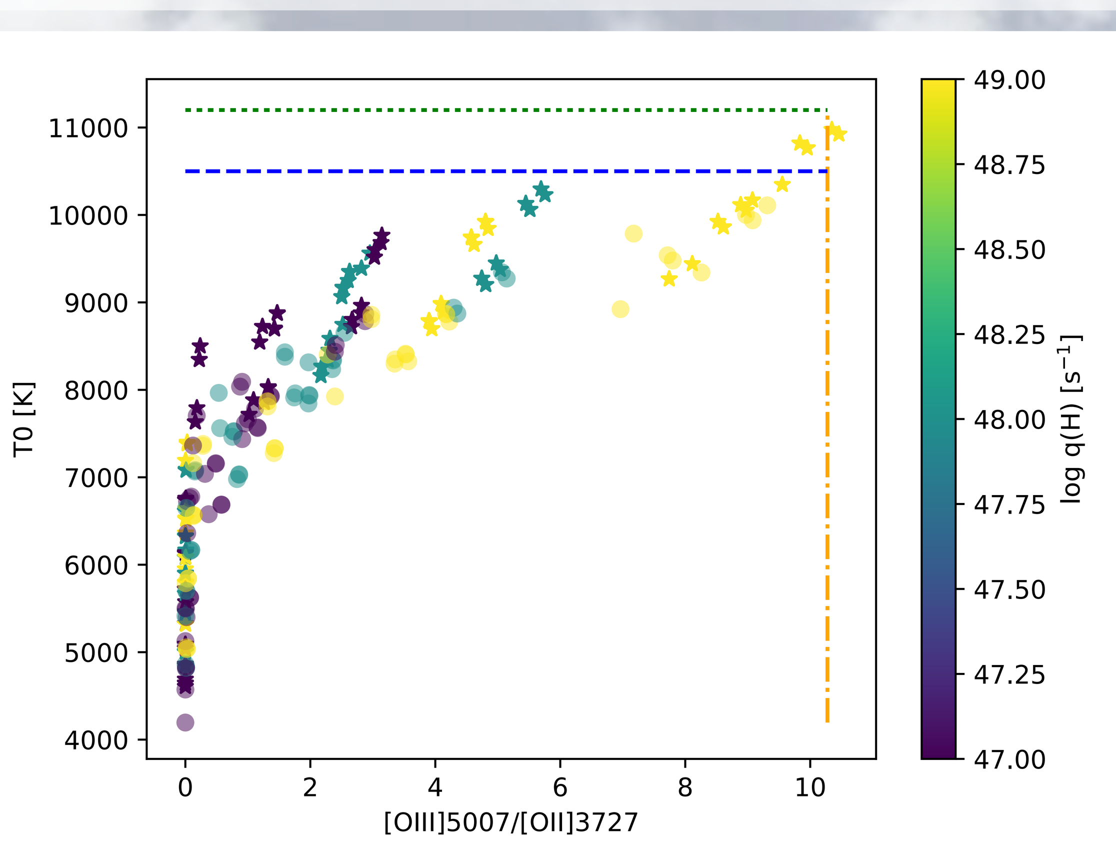

Figure 2. Temperature of the gas as a function of [O III] $\lambda5007$/ [O II] $\lambda3727$. The circles represent the Popstar SED and the stars the Tlusty SED. The symbols are color-coded with the ionization parameter.

SED	Popstar IMF Kroupa
log Q(H) [s^{-1}]	47,48, 49
log R_{in} [cm]	16, 17, 18
log n(H) [cm^{-3}]	2,3
log age [yr]	5.0, 6.4, 6.7
Z_{star}	-3.0, -1.3

SED	Tlusty
log Q(H) [s^{-1}]	47,48, 49
log R_{in} [cm]	16, 17, 18
log n(H) [cm^{-3}]	2,3
T_{eff} [kK]	27.5, 42.5, 55.0
Z_{star}	-2
log g	3.00, 3.75, 4.75

Table 1. Set of parameters for each grid of models.

Results

We selected the model that fitted most of the observed line intensities (Table 2), however, it failed to reproduce the He II lines. To adjust the He II $\lambda4686$ line we modified the spectrum of the ionizing source by adding a power law, that simulates a hard SED (Figure 3). Figure 4 shows the final fit of the model to the observed emission lines.

Parameters	Values
T_{eff} (kK)	40
log Q(H) [s^{-1}]	47
log R_{in} [cm]	17
log n(H) [cm^{-3}]	2
log g	4.75
Metals	0.42
Power law	-1

Table 2. Set of parameters for the final model.

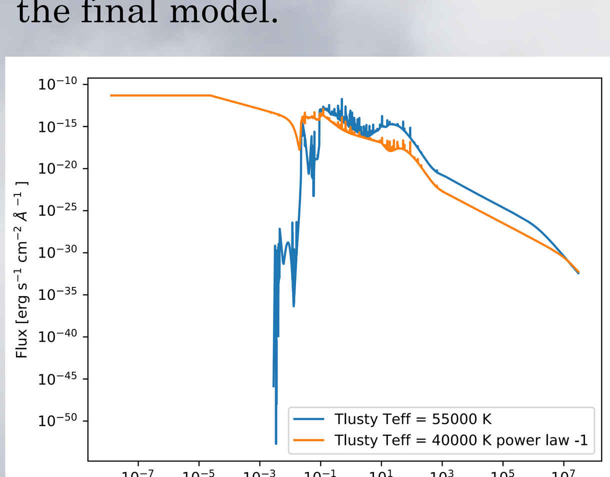

Figure 3. Comparison of the SEDs used in the model.

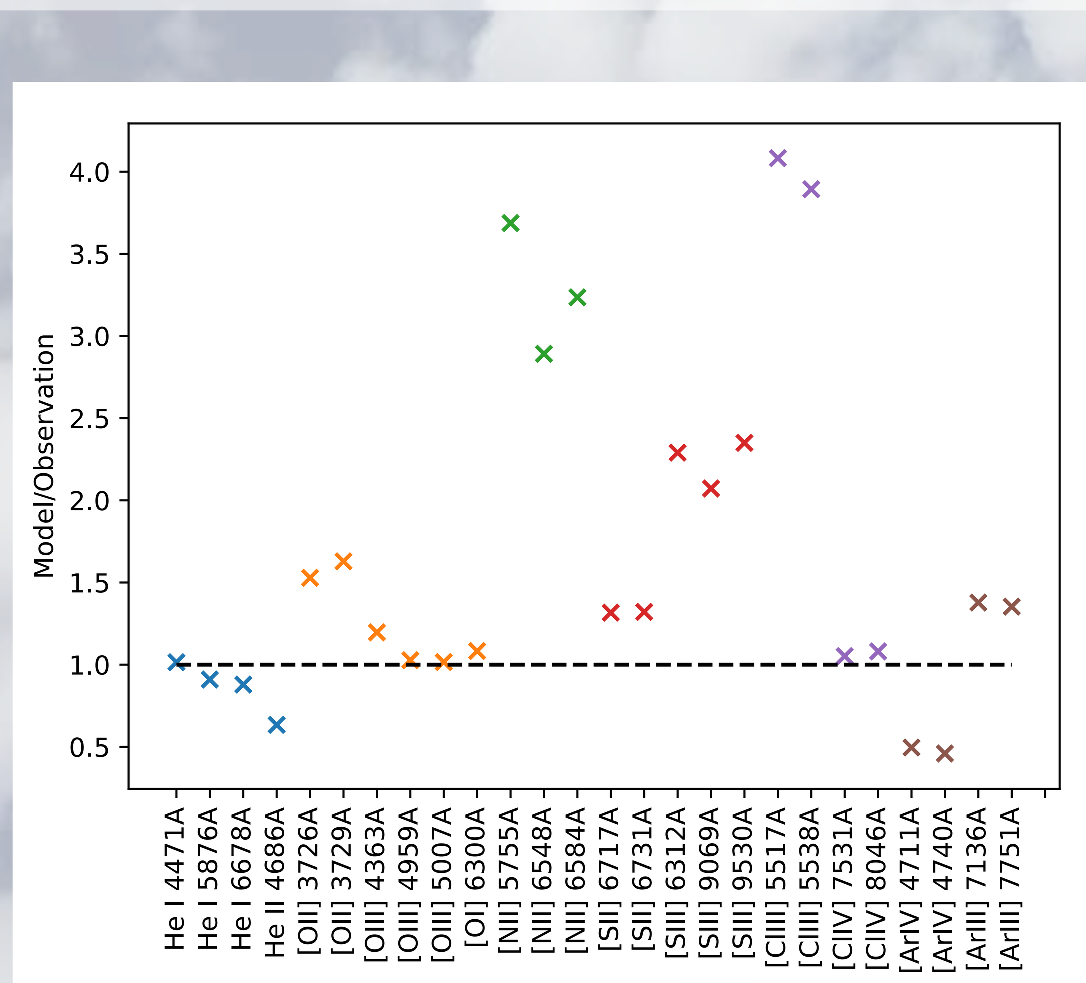

Figure 4. Ratio of the model and observations for different emission lines, each color represents a different element.

The models previously described were also modeled using PyCloudy (Morisset et al 2013). As an interest case, we modeled the line intensity from an H II region, which displayed high density clumps. One of our Popstar grid n_e = 10 cm^{-3} points simulations was repeated with a stop temperature of 8000 K and the transmitted continuum was stored. This spectrum was set as the incident radiation for a second Cloud at n_e = 100 cm^{-3} located at a variable distance from the initial cloud. Using PyCloudy utilities the cloud was converted into a data cube to simulate an sphere. An 1"×50" slit was over imposed these grids to compute the flux passing through. Combining cloudy simulations using different physical conditions with binary and gradient masks and rich set of geometries can be simulated. In our case we defined several high density clumps located in the central region integrating the flux coming from this slit, we calculated the sulfur abundance as with real spectra. Using PyNeb (Luridiana et al. 2016) we calculated the electron density using the diagnostic n_e([S II]) ($\lambda6717/\lambda6730$) and the temperatures using the diagnostics T_e([S III]) (($\lambda9069 + \lambda9531)/\lambda6312$) and T_e([O III]) (($\lambda4959 + \lambda5007)/\lambda4363$). The main ionic fractions were calculated from their emission features intensity. The results can be appreciated in the plot below. While both the initial cloud and the high density clumps have the same metallicity, the measured value is overestimated up-to the 6%.

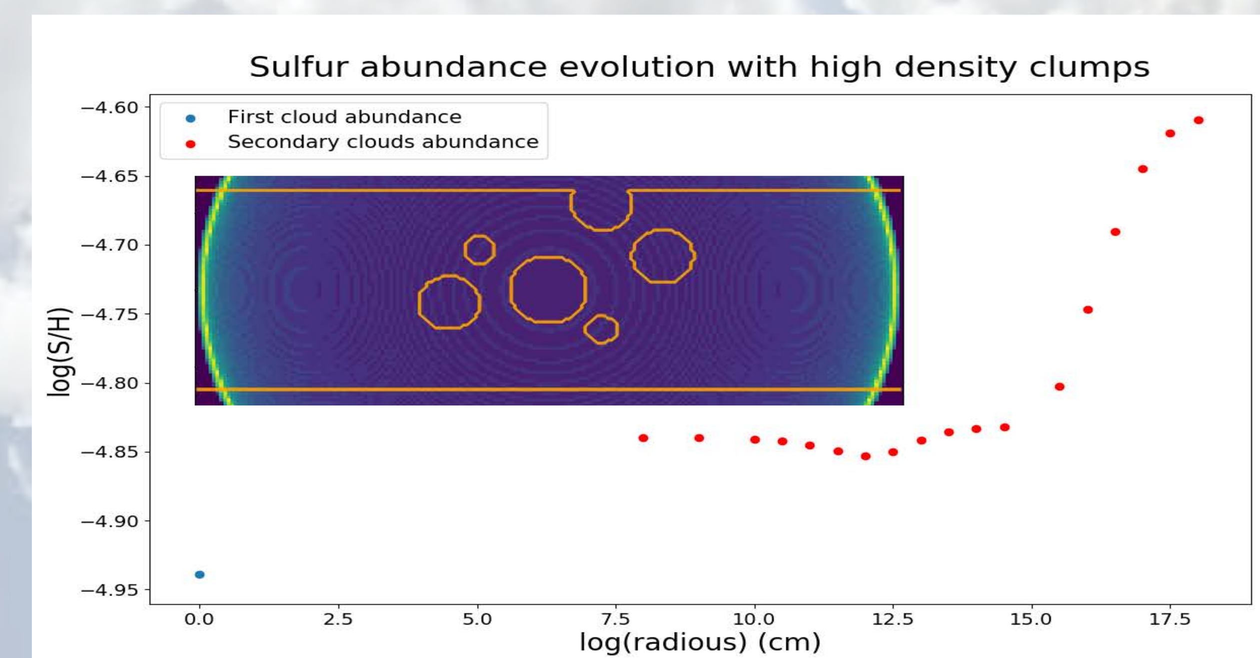

PDR and molecular phase

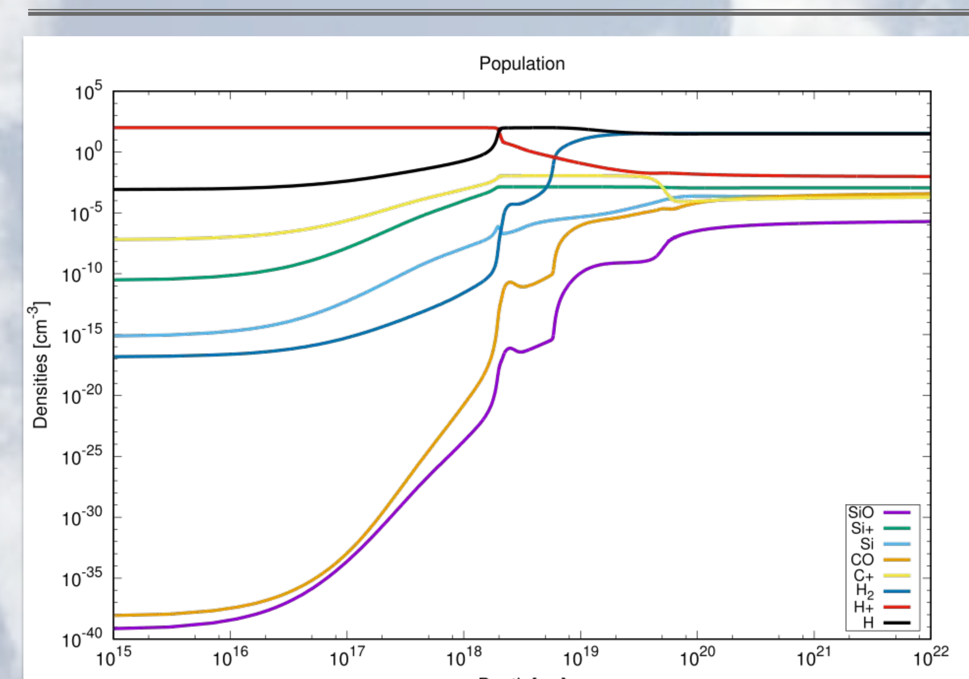

Figure 3. Molecular abundance evolution of HII-PDR-Molecular Cloud with CO, SiO and H2 along physical depth. Within the Large PDR at 10^{17} to 10^{21} cm, molecules are formed while temperature decreases. CO and SiO are formed at almost the same rate.

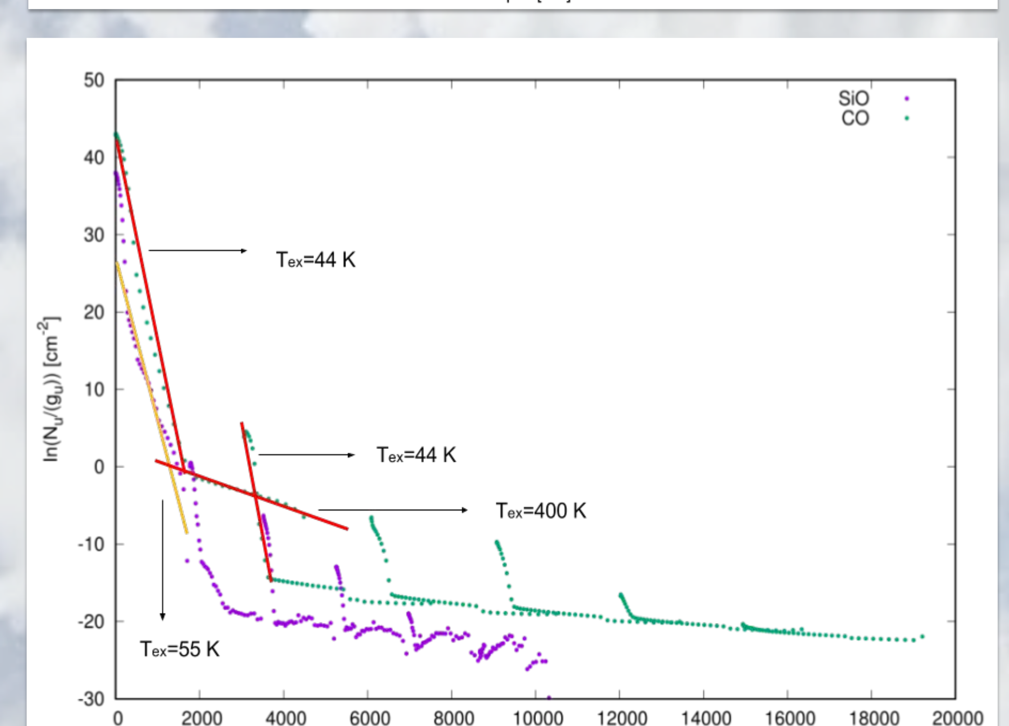

Figure 4. Population diagram of CO and SiO with derived excitation temperatures (level column densities as a function of excitation energies). In optical thick regions, midrange Js have steep drops, while higher rotation levels have higher excitation temperature than lower rotation levels. With the information given, Can you derive vibration temperature?

Conclusions

By constructing a grid of photoionization models to try to reproduce the peculiar object N44C, we have found that:

- The abundance of the He II lines cannot be explained by a single O type star.
- In order to reproduce the observed He II $\lambda4686$ /Hβ = 15.23 (Hβ = 100) it is necessary to add an extra ionization source with a really hard SED.
- Using a photoionization model with an O star and a power law of -1 we can reproduce the overall emission optical lines and particularly the He II line with an average uncertainty of 0.5 dex.
- The higher energy photons needed to reproduce some observed lines suggest that an X-ray source may be present.

Further studies of this object will be necessary to constrain the unknown source of high energy photons.

References

Ferland et al. 2017, 2017arXiv170510877F
Garnett, D. R., Galarza, V. C., & Chu, Y.-H. 2000, ApJ, 545, 251
Lanz, T., & Hubeny, I. 2007, ApJS, 169, 83
Luridiana V., Morisset C., Shaw R. A., 2015, A&A, 573, A42
Morisset, C. 2013, 2013ascl.soft04020M
Martín-Majon et al. 2010, MNRAS, 403, 2012-2032
Nazé Y., Rauw G., Manfroid J., Chu Y.-H., Vreux J.-M., 2003, A&A, 408,171